

RESEARCH ARTICLE



# Yang-Yin-Jie-Du decoction overcomes gefitinib resistance in non-small cell lung cancer via down-regulation of the PI3K/Akt signalling pathway

Shu-yi Chen, Gao-chen-xi Zhang and Qi-jin Shu

Department of Medical Oncology, The First Affiliated Hospital of Zhejiang Chinese Medical University, Hangzhou, Zhejiang, China

## ABSTRACT

**Context:** Yang-Yin-Jie-Du Decoction (YYJDD) was used to improve gefitinib efficacy in our clinical practice, but its mechanism remains unclear.

**Objective:** This study explored if YYJDD could reverse gefitinib resistance.

**Materials and methods:** H1975 cells were exposed to control, 10  $\mu$ M gefitinib, 3.2 mg/mL YYJDD or combination treatment. Cell viability was detected by MTT during 0–96 h. Apoptosis and the PI3K/Akt proteins were tested by flow cytometry and western-blot at 24 h. LY294002 was applied to further determine the role of the PI3K/Akt. 23 BALB/c nude xenograft mice received normal saline ( $n=5$ ), 80 mg/kg gefitinib ( $n=6$ ), 2.35 g/kg lyophilised powder of YYJDD ( $n=6$ ) or combination treatment ( $n=6$ ) by gavage for 4 weeks and submitted to TUNEL, immunohistochemistry, and western-blot.

**Results:** *In vitro*, gefitinib ( $IC_{50}$ :  $20.68 \pm 2.06 \mu$ M) and YYJDD ( $IC_{50}$ :  $6.6 \pm 0.21$  mg/mL) acted in a moderate synergistic way. Combination treatment inhibited cell viability from 100% to 25.66%. Compared to gefitinib ( $33.23 \pm 3.99\%$ ), cell apoptosis was increased with combination treatment ( $54.11 \pm 7.32\%$ ), accompanied by down-regulation of the PI3K/Akt. LY294002 further inhibited cell viability, increased apoptosis, and down-regulated p-Akt/Akt. *In vivo*, the tumour sizes in the combination group ( $1165.13 \pm 157.79$  mm<sup>3</sup>) were smaller than gefitinib alone ( $1630.66 \pm 208.30$  mm<sup>3</sup>). The positive rate of TUNEL staining was increased by combination treatment ( $22.33 \pm 2.75\%$ ) versus gefitinib ( $7.37 \pm 0.87\%$ ), while the PI3K/Akt was down-regulated.

**Discussion and conclusion:** YYJDD has potential to overcome gefitinib resistance. Future investigations should be focussed on its specific targets.

## ARTICLE HISTORY

Received 27 January 2021

Revised 8 July 2021

Accepted 20 August 2021

## KEYWORDS

Chinese herbal medicine; epidermal growth factor receptor-tyrosine kinase inhibitor; lung neoplasm; drug-resistant

## Introduction

Lung cancer is one of the malignant tumours with the highest incidence and mortality rate worldwide. Non-small cell lung cancer (NSCLC), accounting for  $\sim 80\%$ , threatens people's health and lives (Bray et al. 2018). In recent years, the development of the epidermal growth factor receptor tyrosine kinase inhibitors (EGFR-TKIs) has brought new opportunities for the treatment of NSCLC. Due to its advantages of high specificity and low cytotoxicity, EGFR-TKIs have become the first-line agents in the treatment of advanced NSCLC patients harbouring EGFR mutation (Heigener and Reck 2018). Gefitinib, the major representative drug of the first generation of EGFR-TKIs, has been proven that it could prolong the objective response rate (ORR), progression-free survival (PFS), and quality of life in some high-quality clinical trials (Mok et al. 2009; Mitsudomi et al. 2010; Patil et al. 2017). However, most patients will develop drug resistance after 1 year of therapy.

Although the second and third generations of EGFR-TKIs can overcome drug resistance, there still exist some limitations. The side effects of the second generation were more severe than the first, leading to poor tolerance. The price of the third generation is expensive and yet resistance is still inevitable. When suffering from resistance, patients will face dilemmas, such as limited

treatment options. Hence, how to overcome gefitinib resistance is of great significance.

The main reasons for gefitinib resistance include a secondary mutation in EGFR and a relevant signalling pathway (Normanno et al. 2017). The phosphatidylinositol 3-kinase (the PI3K)/protein kinase B (Akt) signalling pathway is a classical downstream signal molecule of EGFR and is considered a pivotal pathway in carcinogenesis. Previous studies have confirmed that EGFR secondary mutation, bypass activation, or induced-angiogenesis can drive the PI3K/Akt pathway (Gendreau et al. 2007; Turke et al. 2010; Larsen et al. 2011). The PI3K can act as an important inducer of EGFR-TKI resistance in NSCLC (Marędziaik et al. 2017). Moreover, down-regulation of the PI3K/Akt signalling pathway has been authenticated to reverse EGFR-TKI resistance in recent research (Wu et al. 2015; Sato et al. 2018). Therefore, the PI3K/Akt pathway plays a critical role in EGFR-TKI resistance.

As one important strategy to overcome EGFR-TKIs resistance, Chinese herbal medicine (CHM) has become a research highlight. Both clinical and basic investigations have confirmed that CHM has significant advantages in overcoming drug resistance (Li et al. 2016; Jiao et al. 2019). In clinical observation, patients who suffer from gefitinib resistance always present the symptoms of dryness-heat, thirst, night sweat, constipation, etc. Yang-Yin-

Jie-Du Decoction (YYJDD) was formulated by Professor Qijin Shu, a famous doctor of traditional Chinese medicine in Zhejiang Province, based on his years of clinical experience. It consists of Radix *Glehnia littoralis* F. Schmidt ex Miq. (Apiaceae) [Beishashen], Radix *Ophiopogon japonicus* (L. f.) Ker-Gawl. (Asparagaceae) [Maidong], Bulbus *Lilium brownii* var. *viridulum* Baker (Liliaceae) [Baihe], Caulis *Dendrobium nobile* Lindl. (Orchidaceae) [Shihu], Herba *Hedyotis diffusa* Willd. (Rubiaceae) [Baihuasheshicao], Cacumen *Taxus wallichiana* var. *mairei* (Lemée & H. Lév.) L. K. Fu & Nan Li (Taxaceae) [Nanfanghongdoushan], Pericarpium *Citrus reticulata* Blanco (Rutaceae) [Chenpi] and Radix *Codonopsis pilosula* (Franch.) Nannf. (Campanulaceae) [Dangshen]. The main function is to treat patients with the above symptoms after taking EGFR-TKIs. In our daily clinical practice, we found that YYJDD could reduce the side effects of EGFR-TKIs, improve the life quality of patients and prolong their PFS (Li 2017). Pre-experiment also revealed that YYJDD combined with gefitinib could inhibit the growth of drug-resistant cell line *in vitro*. But its mechanism still remains unclear. Therefore, we concentrate on the effect of YYJDD combined with gefitinib on NCI-H1975 cells (gefitinib-resistant cell line) and explore the underlying molecular mechanism *in vitro* and *in vivo*.

## Materials and methods

### YYJDD preparation

YYJDD is a mixture of *G. littoralis*, *O. japonicus*, *L. brownii* var. *viridulum*, *D. nobile*, *H. diffusa*, *T. wallichiana* var. *mairei*, *C. reticulata*, and *C. pilosula* at a mass ratio of 15:15:12:12:8:12:15. They were purchased from the Chinese Pharmacy of the First Affiliated Hospital of Zhejiang Chinese Medical University (Hangzhou, Zhejiang, China). The CHM formula was soaked for 30 min and extracted with 100 °C water 3 times. As it was filtered by a vacuum coolant, the decoction was concentrated with a rotary evaporator. Then the concentrated extract was lyophilised to obtain powder (yield: 17.4%) and stored at -80 °C. Before the *in vitro* experiment, the lyophilised powder was dissolved in cell culture medium and centrifuged at 15 000 rpm for 5 min. Then the resulting supernatant was filtered with a 0.22 µm sterile filter. After YYJDD was added into the medium, the pH value was adjusted to 7.2–7.4. For *in vivo* experiments, animals were treated with intragastric administration when the powder was dissolved in physiological saline.

### High-performance liquid chromatography (HPLC) analysis

HPLC analysis was performed by using Agilent 1260 HPLC system (Agilent Technologies, Santa Clara, CA) and the analytes were separated on the Agilent Zorbax SB C18 column (4.6 mm × 150 mm, 5 µm, Agilent Technologies, Santa Clara, CA). Samples with a volume of 10 µL were injected into the column for separation and the column temperature remained at 25 °C. The flow rate was 1 mL/min. The mobile phase included solvents A (pure water) and B (acetonitrile). The gradient elution program was set as follows: 0–30 min, 5–50% B; 30–50 min, 50–100% B; 50–53 min, 100% B; 53–55 min, 100–5% B; 55–57 min, 5% B. Reference solutions of 6- $\alpha$ -hydroxygeniposide, hesperidin, lobetyolin, dioscin, and sciadopitysin were purchased from Chengdu Herbpurify Co., Ltd. (Sichuan, China).

### Cell culture

NCI-H1975 cells harbouring EGFR-L858R/T790M mutant were resistant to gefitinib. The cell line was purchased from the Chinese Academy of Science Cell Bank (Shanghai, China). Cells were cultured in Dulbecco's modified Eagle's medium (DMEM) supplemented with 10% foetal bovine serum (FBS), 1 mM glutamine and 1% penicillin/streptomycin. The cell cultures were maintained at 37 °C in a humidified atmosphere of 5% CO<sub>2</sub>.

### Cell viability assay

To test the efficacy of YYJDD and gefitinib (Xianyu Technology Co., Ltd., Hubei, China) on the growth of H1975 cells, cells were incubated in DMEM containing 0, 2, 4, 6, 8, 12, 16 mg/mL YYJDD and 0, 2, 4, 8, 12, 16, 24, 32, 40 µM gefitinib separately for 24 h. Then the half-maximal inhibitory concentration (IC<sub>50</sub>) values of YYJDD and gefitinib were calculated. The interaction between YYJDD and gefitinib was evaluated by using the Chou-Talalay method (Chou 2006, 2010). The antiproliferative effects of YYJDD, gefitinib, and combination treatment on H1975 cells were tested at the doses of 0, 0.125, 0.25, 0.5, 1, 2, and 4 times IC<sub>50</sub> values. Then the combination index (CI) was calculated by Calcsyn software to identify whether synergism existed between gefitinib and YYJDD. Afterwards, the cells were exposed to gefitinib, YYJDD and combination treatment for 0, 24, 48, 72, and 96 h in order to explore the inhibitory effects on the cell viability at different time points. MTT assay was performed to assess the cytotoxicity according to the manufacturer's protocol. Briefly, 8 × 10<sup>3</sup> H1975 cells were seeded in 96-well plates for 24 h. After exposure, each well was added with 50 µL of MTT solution (1 mg/mL, Sigma-Aldrich, St. Louis, MO, USA) and incubated for 3 h. Finally, 150 µL of DMSO was added to each well, and the plates were shaken for 10 min for crystal dissolution. The optical density (OD) at 570 nm was determined by Multiskan MK3 Microplate Reader (Thermo Scientific, MA, USA). In all MTT assays, blank control without cells was run in parallel. The cell survival rate was calculated as follows:

$$\text{Cell survival rate (\%)} = \frac{(\text{OD}_{\text{sample}} - \text{OD}_{\text{blank}})}{(\text{OD}_{\text{control}} - \text{OD}_{\text{blank}})} \times 100\%$$

### Cell apoptosis assays

Annexin V-FITC/PI double staining apoptosis detection kit (4 A Biotech Co., Ltd, Beijing, China) was used to test the cell apoptosis. Briefly, 5 × 10<sup>5</sup> cells were incubated in each petri dish (diameter: 6 cm) for 24 h and then exposed to 10 µM gefitinib, 3.2 mg/mL YYJDD, or combination treatment for further 24 h. Subsequently, the cells were collected with trypsin and washed with ice-cold PBS for 2 times. Then 1 × binding buffer was used to re-suspend the cells and the concentration was adjusted to 1 × 10<sup>6</sup> cells/mL. The cells were stained with 5 µL Annexin V-FITC and 10 µL PI at room temperature in dark for 10 min. The data of apoptotic cells were analysed by Attune™ NxT Flow Cytometer (Invitrogen, CA, USA).

### Western blot analysis

Cells and tumour tissues were lysed with RIPA buffer containing 1 mM phenylmethylsulfonyl fluoride (PMSF) and phosphatase inhibitor (Beyotime, Shanghai, China). Pierce™ BCA protein

assay kit (Thermo Scientific, IL, USA) was applied to quantify the concentrations of proteins. The same number of proteins were solubilised in 2× sodium dodecyl sulphate (SDS) sample buffer and resolved on 10% sodium dodecyl sulphate-polyacrylamide gel electrophoresis (SDS-PAGE). Afterwards, they were transferred to polyvinylidene fluoride (PVDF) membranes (0.45 µm, Millipore, Darmstadt, Germany). The membranes were blocked with 5% skim milk for 2 h and then incubated with primary antibodies at 4 °C overnight. The primary antibodies applied in this study were as follows: cleaved caspase-3, cleaved PARP, PI3K, p-PI3K, Akt, p-Akt, and β-actin (Cell Signalling Technology, MA, USA). Subsequently, the membranes were washed and incubated with appropriate horseradish peroxidase (HRP)-conjugated secondary antibodies at room temperature for 2 h. Signals were measured by an enhanced chemiluminescence (ECL) kit (Bio-Rad, CA, USA) and analysed by Image J software.

### Inhibition of the PI3K/Akt pathway

To further investigate the role of the PI3K/Akt pathway on YYJDD overcoming gefitinib resistance, H1975 cells were pre-treated with 10 µM LY294002 (10 mM, Selleckchem, TX, USA) for 30 min followed by exposure to 3.2 mg/mL YYJDD combined with or without 10 µM gefitinib for further 24 h. Cell viability, cell apoptosis, and expressions of Akt and p-Akt proteins were determined by MTT assay, flow cytometry analysis, and western blot, respectively. The specific experimental processes were in the light of the above approaches.

### Animal ethical approval

All *in vivo* experiments were conducted in strict accordance with applicable national and institutional guidelines on the use and care of laboratory animals. The protocol was approved by the University Ethical and Welfare Committee for Animal Experiments (Approval No. IACUC-20200921-03).

### Nude mice transplantation tumor model

BALB/c nude mice (3–5 weeks old) were purchased from Sino-British SIPPR/BK Laboratory Animal Ltd (Shanghai, China). The mice were maintained in a dedicated Specific Pathogen Free (SPF) facility. Cell suspension (0.2 mL) containing  $4 \times 10^6$  NCI-H1975 cells was subcutaneously transplanted with each mouse. According to the dose conversion table between human and animal (Wei et al. 2010), the ratio of mouse dose to human dose was 9.1:1. In addition, the yield of YYJDD was 17.4%. After calculation, the dose of YYJDD lyophilised powder was determined as 2.35 g/kg. The dose of gefitinib was determined according to the previous publication (Liu et al. 2014). When the tumour mass reached  $\sim 80 \text{ mm}^3$ , 23 mice were randomly divided into 4 groups and treatments were began by intragastric administration once a day as follows: control group ( $n = 5$ ): equal volume of saline; gefitinib group ( $n = 6$ ): 80 mg/kg gefitinib; YYJDD group ( $n = 6$ ): 2.35 g/kg lyophilised powder of YYJDD; combination group ( $n = 6$ ): 80 mg/kg gefitinib + 2.35 g/kg YYJDD. The tumour volume and the body weight of each mouse were measured every other day for four consecutive weeks. Finally, all the mice were sacrificed and the tumours were collected. The tumour volume of each mouse was calculated according to the following formula:

$$\text{Tumour Volume} = \pi/6 \times \text{Length} \times \text{Width} \times \text{Height}.$$

### TUNEL staining

TUNEL Apoptosis Detection Kit (Alexa Fluor 488, Yeasen Biotech Co., Ltd., Shanghai, China) was applied to detect apoptosis *in vivo* on the basis of the manufacturer's instructions. Briefly, the sections of tumour tissues were deparaffinized in xylene and rehydrated in PBS buffer. Each sample was added with 20 µg/mL proteinase K and incubated at 37 °C for 20 min. After being washed with PBS buffer for 3 times, the sections were incubated in 1× equilibration buffer for 30 min and then with 50 µL TUNEL reaction mixtures (34 µL ddH<sub>2</sub>O + 10 µL 5× Equilibration Buffer + 5 µL Alexa Fluor 488-12-dUTP Labelling Mix + 1 µL Recombinant TdT Enzyme) in a wet box for 1 h at 37 °C in the dark. Subsequently, the sections were washed with PBS buffer 3 times. 2-(4-Aminophenyl)-6-indolecarbamidine dihydrochloride (DAPI) Staining Solution (Beyotime, Shanghai, China) was added to stain the nucleus and incubated in dark for 5 min. The slides were observed by the fluorescence microscope (Nikon, Tokyo, Japan).

### Immunohistochemical analysis

Tumour tissues of mice were harvested, dehydrated, paraffin-embedded and incubated with the primary antibody at 4 °C overnight. The primary antibodies used in this study including Ki-67 and p-Akt (Cell Signalling Technology, MA, USA). After being washed with PBS for 3 times, the sections were incubated with HRP conjugated secondary antibodies at 37 °C for 20 min. Then, diaminobenzidine (DAB) solution was used to stain the slice and the nuclei were counterstained with Harris' haematoxylin. Finally, sections were imaged on an optical microscope (Nikon, Tokyo, Japan). H-score involved a semi-quantitative assessment of positive cell percentage and staining intensity. Staining intensity was scored within a scale ranging from 0 to 300, and categorised as follows: no staining, 0; weak staining, 1<sup>+</sup> (light brown); intermediate staining, 2<sup>+</sup> (brown); and strong staining, 3<sup>+</sup> (dark brown). The outcomes were calculated as the following formula:

$$\text{H-score} = 1 \times (\% \text{ of } 1^+ \text{ cells}) + 2 \times (\% \text{ of } 2^+ \text{ cells}) + 3 \times (\% \text{ of } 3^+ \text{ cells}).$$

### Statistical analysis

All graphs, calculations and statistical analyses were performed with GraphPad Prism software version 5.0. Data measurement was expressed as mean ± standard deviation (SD) of at least 3 independent experiments. Statistical comparisons were determined by a one-way or two-way ANOVA test.  $P < 0.05$  was considered as statistical significance.

## Results

### Chemical composition of YYJDD

HPLC was performed to identify YYJDD, revealing 5 major chemical compounds: hesperidin, sciadopitysin, dioscin, 6- $\alpha$ -hydroxygeniposide and lobetyolin (Figure 1). The content of each identified ingredient in the aqueous extract of YYJDD was shown in Table 1. Its stability and repeatability were guaranteed.

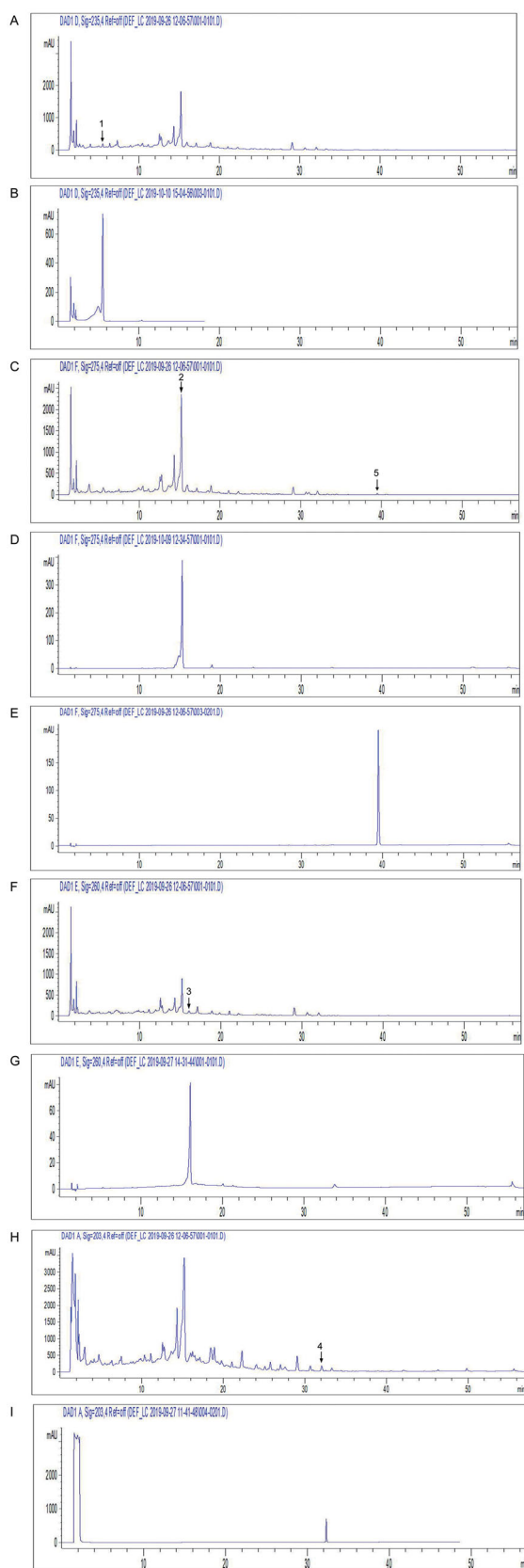


**Figure 1.** Aqueous extractions of YYJDD were qualitatively analysed by HPLC. The numbers in the chromatograms showed the constituent peaks. (A) Peak 1 was identified as 6- $\alpha$ -hydroxygeniposide. (B) Reference standard substance of 6- $\alpha$ -hydroxygeniposide. (C) Peak 2 was identified as hesperidin and peak 5 was sciadopitysin. (D) Reference standard substance of hesperidin. (E) Reference standard substance of sciadopitysin. (F) Peak 3 was identified as lobetyolin. (G) Reference standard substance of lobetyolin. (H) Peak 4 was identified as dioscin. (I) Reference standard substance of dioscin. A typical chromatogram was shown ( $n = 3$ ).

**Table 1.** Content of each identified ingredient in aqueous extract of YYJDD.

Components	Content (mg/g)
6- $\alpha$ -Hydroxygeniposide	14.90 $\pm$ 0.33
Hesperidin	156 $\pm$ 31.98
Lobetyolin	9.22 $\pm$ 0.28
Dioscin	3.66 $\pm$ 0.040
Sciadopitysin	0.69 $\pm$ 0.11

### Effects of YYJDD combined with gefitinib on growth of H1975 cells

The H1975 cell line, which harbours EGFR mutations of exon 21 L858R and exon 20 T790M, was selected in our study as it is resistant to the first generation of EGFR-TKI. Gefitinib, the first generation of EGFR-TKI, is a small molecule inhibitor that targets EGFR tyrosine kinase activity. Firstly, we examined the inhibitory effect of gefitinib and YYJDD on H1975 cells by MTT assay at 24 h. The  $IC_{50}$  values of gefitinib and YYJDD were  $20.68 \pm 2.06 \mu\text{M}$  and  $6.6 \pm 0.21 \text{ mg/mL}$ , respectively (Figure 2(A,B)). Then, the cell proliferation assay was performed to identify the synergistic effect of gefitinib and YYJDD on H1975 cells. Figure 2(C,D) indicated the combined drug effect of gefitinib and YYJDD, which was shown as fractional cell growth inhibition (FA) as a function of CI. Table 2 showed CI values of 20, 50, and 80% cytotoxicity (FA = 0.2, 0.5, 0.8, respectively). The CI value of gefitinib combined with YYJDD was less than 0.85 (mean CI at  $FA_{0.5} = 0.846$ ), illustrating that there was a moderate synergistic effect between the two drugs to inhibit growth. When the growth of 50% cells was inhibited, the concentrations of gefitinib and YYJDD were  $10 \mu\text{M}$  and  $3.2 \text{ mg/mL}$ , respectively. Hence, the above drug doses were used in the following experiments. We further explored the inhibitory effects of combination treatment (YYJDD plus gefitinib) on the cell viability at different time points (0, 24, 48, 72, and 96 h). Compared with the control group at 0 h, the cell survival rates of the combination group at 24, 48, 72, and 96 h were  $77.14 \pm 4.73\%$ ,  $63.95 \pm 5.08\%$ ,  $41.20 \pm 5.48\%$ , and  $25.66 \pm 3.14\%$ , respectively. At any time point, the cell viability of the combination group was significantly lower than that of the control or gefitinib group at the same time ( $p < 0.05$ ). Thus, cell proliferation was greatly inhibited in the combination group in a time-dependent manner (Figure 2(E)). These results indicated that YYJDD could enhance the gefitinib-induced inhibitory effect on the growth of H1975 cells.

### YYJDD enhanced the efficacy of gefitinib to induce cell inhibition via apoptosis

Cell proliferation assay certified that YYJDD combined with gefitinib could promote cell inhibition in H1975 cells, so we endeavoured to determine whether the decrease of cell number was related to apoptosis. The flow cytometry was applied to measure the effect of combination treatment on apoptosis. The results revealed that gefitinib alone slightly induced cell apoptosis, while the increasing apoptosis cells were detected in the combination group ( $33.23 \pm 3.99\%$  vs.  $54.11 \pm 7.32\%$ ,  $p < 0.01$ ) (Figure 3(A,B)). To further determine the pro-apoptotic effect of YYJDD combined with gefitinib in H1975 cell line, we used western blot to detect the apoptosis-related proteins. As shown in Figure 3(C–E), the expressions of cleaved caspase-3 and cleaved PARP were further increased in the presence of combination treatment

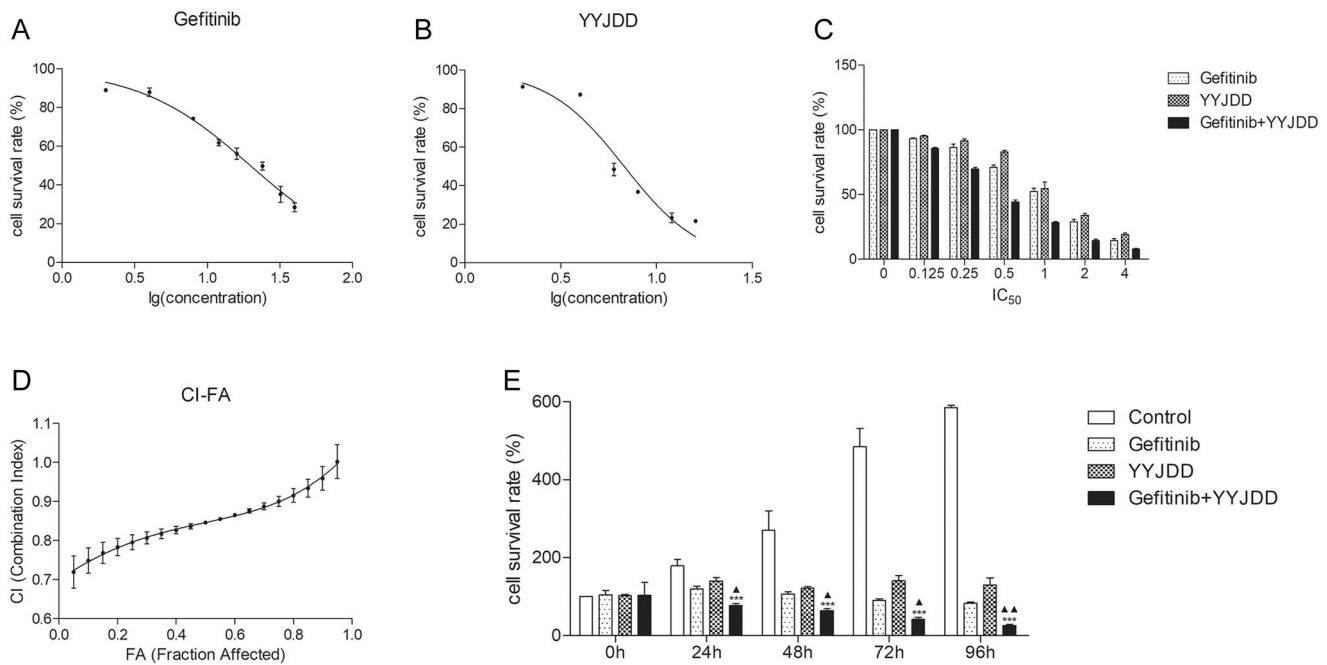


**Figure 2.** There was a moderate synergistic effect between gefitinib and YYJDD to inhibit the growth of H1975 cells. (A) H1975 cells were treated with different concentrations of gefitinib (2, 4, 8, 12, 16, 24, 32, 40  $\mu$ M) for 24 h. Then, the cell viability was measured by MTT assay and  $IC_{50}$  of gefitinib was calculated. (B) H1975 cells were exposed to different concentrations of YYJDD (2, 4, 6, 8, 12, 16 mg/mL) for 24 h. Then, the cell survival rate was tested by MTT assay and  $IC_{50}$  of YYJDD was calculated. (C) H1975 cells were exposed to gefitinib, YYJDD, and combination treatment at the doses of 0.125, 0.25, 0.5, 1, 2, and 4 times  $IC_{50}$  values. Then, MTT assay was performed to evaluate the viability of cells. (D) Combined Index (CI) values at different levels of growth inhibition effect (fraction affected, FA) were calculated by Calcsyn software to analyse the synergism between gefitinib and YYJDD. (E) H1975 cells were exposed to gefitinib, YYJDD, and combination treatment for 24, 48, 72, and 96 h. MTT assay was applied to assess the cytotoxicity. Data were represented as mean  $\pm$  SD. All experiments were done in triplicate. \*\*\* $p < 0.001$  compared with control,  $\blacktriangle p < 0.05$ ,  $\blacktriangle\blacktriangle p < 0.01$  compared with gefitinib.

**Table 2.** Summary of CI values at 20, 50, and 80% FA.

Regimen	CI at FA(%)		
	20	50	80
Gefitinib + YYJDD	0.7830 $\pm$ 0.0221	0.8460 $\pm$ 0.0036	0.9153 $\pm$ 0.0172

CI: Combined Index; FA: Fraction Affected; Data were represented as mean  $\pm$  SD of three independent experiments.

versus control or gefitinib group. Taken together, these data indicated that gefitinib combined with YYJDD could significantly up-regulate pro-apoptotic proteins and induce apoptosis in H1975 cells.

### YYJDD combined with gefitinib induced cell apoptosis through inactivating the PI3K/Akt pathway

Given that the PI3K/Akt signalling pathway was associated with gefitinib resistance, we detected the level of PI3K, p-PI3K, Akt, and p-Akt by western-blot analysis. As shown in Figure 4(A–C), the ratio of p-PI3K/PI3K and p-Akt/Akt were slightly decreased by the intervention of gefitinib, while YYJDD or the combination treatment significantly down-regulated the ratio of these proteins.

It has been confirmed that LY294002, an inhibitor of the PI3K/Akt signalling pathway, can enhance the sensitivity of H1975 cells to gefitinib (Li et al. 2011). Therefore, the PI3K/Akt pathway plays a vital role in the mechanism of gefitinib resistance (Ludovini et al. 2011). To further confirm the role of the PI3K/Akt pathway in the combination treatment-mediated apoptosis, H1975 cells were pre-treated with LY294002 before exposure to YYJDD or combination treatment. MTT, flow cytometry,

and western blot assay were performed. As shown in Figure 4(D–F), compared to YYJDD alone, the addition of LY294002 enhanced the effect of YYJDD on cell growth ( $79.48 \pm 2.06\%$  vs.  $40.01 \pm 1.96\%$ ,  $p < 0.001$ ) and apoptosis ( $17.81 \pm 1.88\%$  vs.  $47.20 \pm 1.84\%$ ,  $p < 0.001$ ). Meanwhile, the influence of combination treatment on cell growth ( $49.84 \pm 2.45\%$  vs.  $24.36 \pm 1.17\%$ ,  $p < 0.001$ ) and apoptosis ( $50.26 \pm 5.39\%$  vs.  $68.40 \pm 3.63\%$ ,  $p < 0.001$ ) of H1975 was further strengthened in the presence of LY294002. Additionally, LY294002 decreased cell viability and promoted apoptosis, not only alone but also in the presence of YYJDD or combination treatment. According to the results of western-blot analysis, the ratio of p-Akt/Akt in H1975 cells was significantly decreased by YYJDD or combination treatment, which was further reduced in the presence of LY294002. That is to say, LY294002 enhanced the effect of both YYJDD and combination treatment on the protein expression ratio of p-Akt/Akt. Furthermore, the presence of YYJDD or combination treatment could further decrease the ratio of p-Akt/Akt induced by LY294002 (Figure 4(G,H)). These data suggested that the cell proliferation inhibition and apoptosis induced by YYJDD combined with gefitinib were dependent on the PI3K/Akt signalling pathway.

### YYJDD reduced gefitinib resistance via the PI3K/Akt pathway in NSCLC in vivo

The above *in vitro* experiments proved that YYJDD could enhance the efficacy of gefitinib on H1975 cells, which was dependent on the PI3K/Akt pathway. To analyse whether YYJDD could reduce gefitinib resistance *in vivo*, we used a xenograft tumour model by transplanting H1975 cells to BALB/c

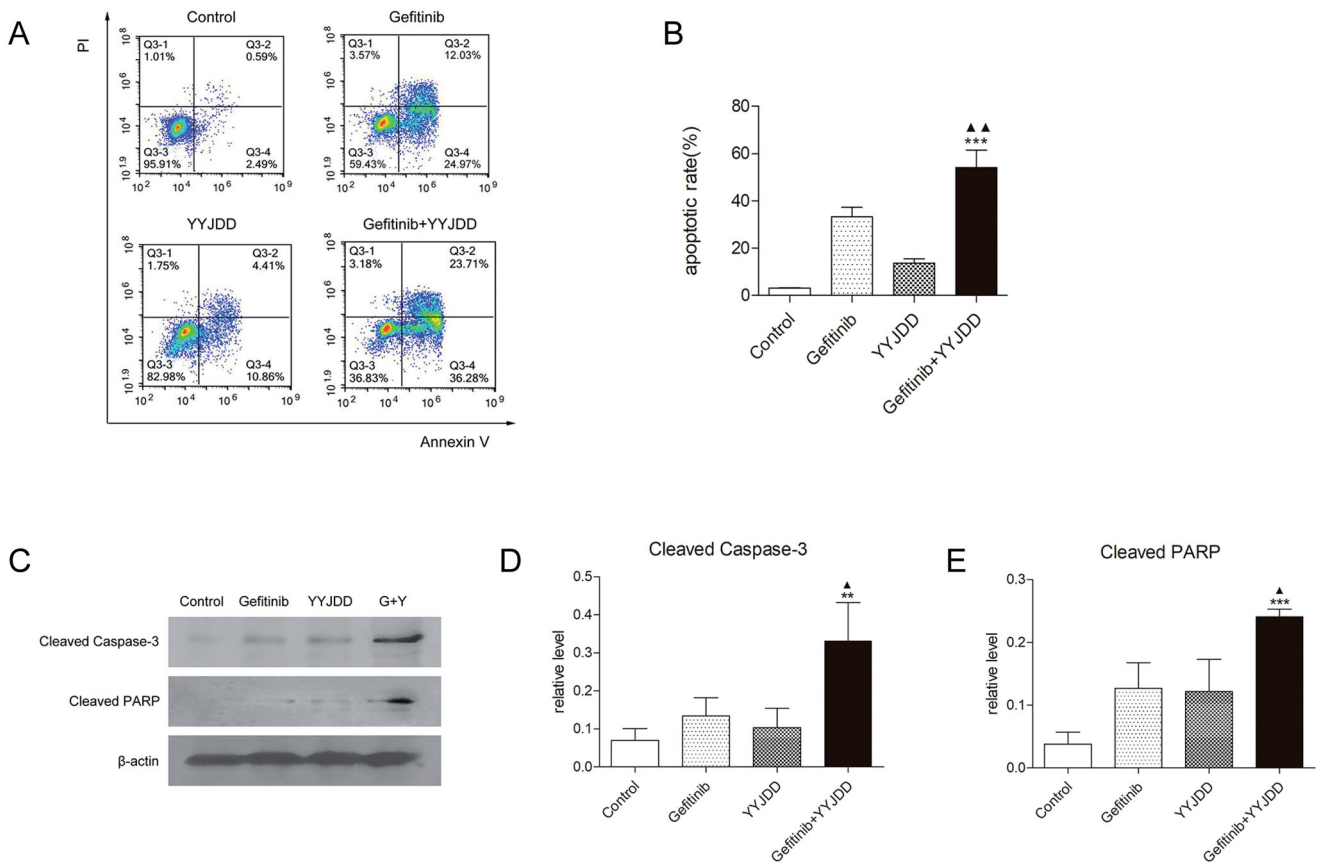


**Figure 3.** YYJDD enhanced gefitinib-induced apoptosis in H1975 cells. H1975 cells were exposed to gefitinib, YYJDD and combination treatment for 24 h. (A, B) Cells were stained with Annexin V-FITC/PI. The rate of apoptotic cells was detected by flow cytometry. The apoptotic rate was calculated. X-axis: the level of Annexin-V FITC fluorescence; Y-axis: the PI fluorescence. (C) The protein expressions of cleaved caspase-3 and cleaved PARP were analysed by western-blot.  $\beta$ -actin was used as an internal control. (D, E) The relative protein expressions of cleaved caspase-3 (D) and cleaved PARP (E) were quantified by normalising to  $\beta$ -actin and statistically analysed. Data was reported as the mean  $\pm$  SD. All experiments were performed three times. \* $p < 0.01$ , \*\* $p < 0.001$  versus control, and  $\blacktriangle p < 0.05$ ,  $\blacktriangle\blacktriangle p < 0.01$  versus gefitinib group. G: Gefitinib; Y: YYJDD.

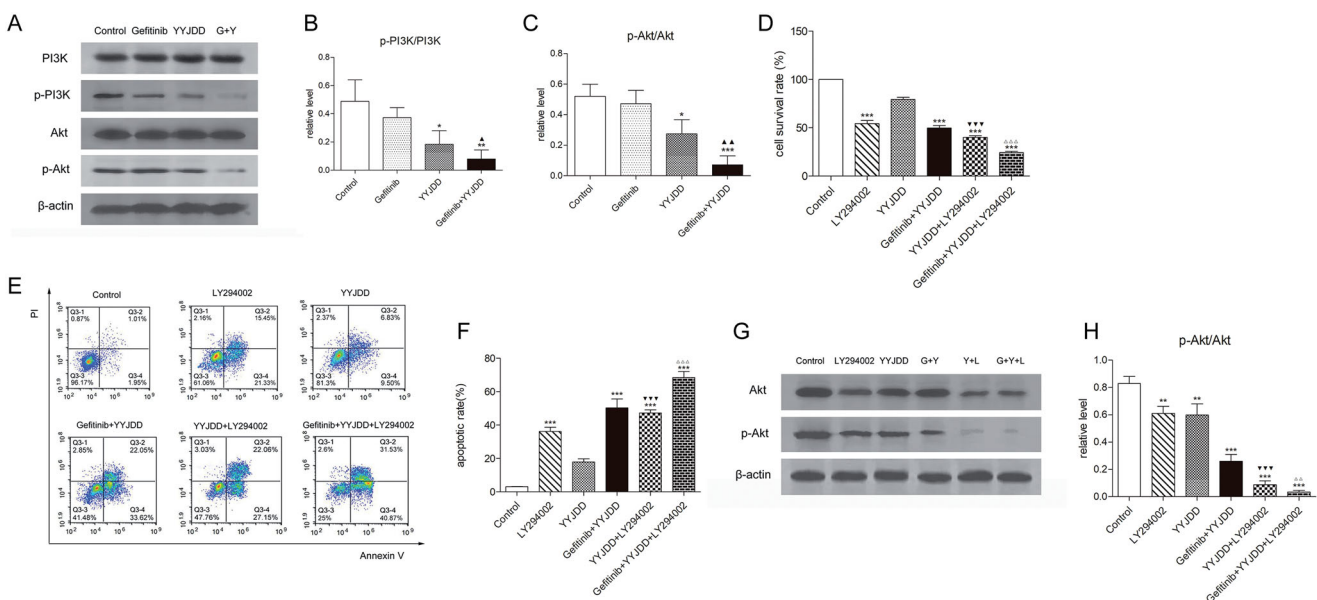


**Figure 4.** YYJDD reversed gefitinib resistance in H1975 cells via down-regulation of the PI3K/Akt signalling pathway. (A) H1975 cells were treated with gefitinib, YYJDD and combination therapy for 24 h. Then, the protein expressions of PI3K, p-PI3K, Akt and p-Akt were determined by western-blot.  $\beta$ -actin was used as an internal control. (B, C) The relative level of p-PI3K/PI3K (B) and p-Akt/Akt (C) were statistically analysed. (D) H1975 cells were pre-treated with LY294002, and then co-treated with YYJDD and combination therapy for a further 24 h. Cell viability was analysed by MTT assay. (E, F) Cell apoptosis was detected by flow cytometry. The apoptotic rate was calculated. X-axis: the level of Annexin-V FITC fluorescence; Y-axis: the PI fluorescence. (G) The protein expressions of Akt and p-Akt were determined by western-blot.  $\beta$ -actin was used as an internal control. (H) The relative level of p-Akt/Akt was statistically analysed. Data were presented as mean  $\pm$  SD of three independent tests. \* $p < 0.05$ , \*\* $p < 0.01$  and \*\*\* $p < 0.001$  versus control;  $\blacktriangle p < 0.05$ ,  $\blacktriangle\blacktriangle p < 0.01$  versus gefitinib group;  $\blacktriangledown\blacktriangledown\blacktriangledown p < 0.001$  versus YYJDD;  $\triangle\triangle\triangle p < 0.01$ ,  $\triangle\triangle\triangle\triangle p < 0.001$  versus gefitinib plus YYJDD. G: Gefitinib; Y: YYJDD; L: LY294002.

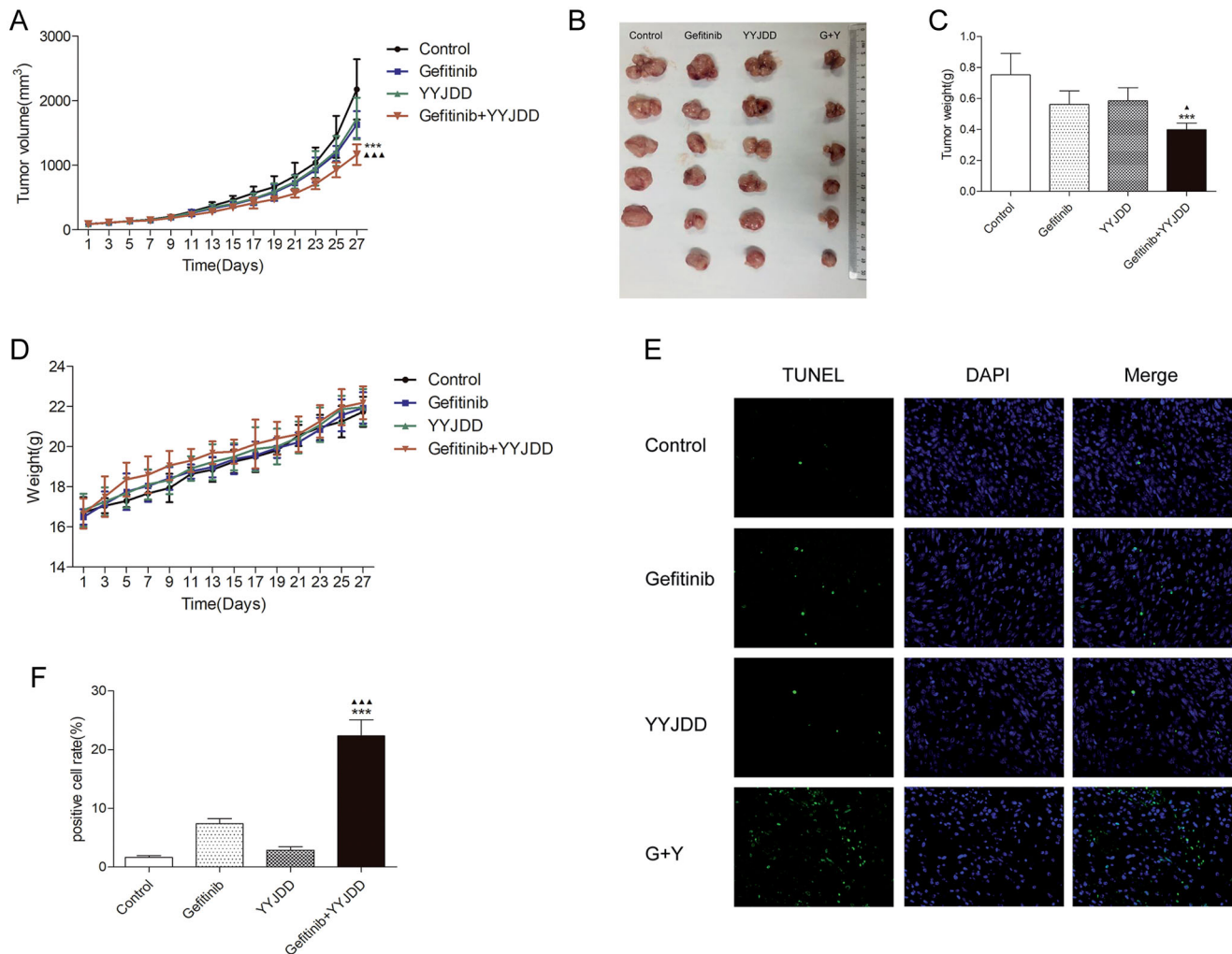


**Figure 5.** YYJDD overcame gefitinib resistance *in vivo*. H1975 cells were transplanted to BALB/c nude mice. The mice were randomly divided into four groups: control, gefitinib, YYJDD, and gefitinib + YYJDD group. (A) Tumour volumes of mice were measured every other day for 4 consecutive weeks. (B) The nude mice were sacrificed at the end of the 4th week and the tumours were collected. (C) The tumour tissues were weighed and calculated. (D) The body weights of mice were measured every other day for 4 consecutive weeks. (E) Apoptosis in tumour tissues was detected by TUNEL staining (original magnification,  $\times 400$ ). Green fluorescence indicated TUNEL staining; Blue fluorescence indicated DAPI staining. (F) TUNEL positive cell rate in each group was calculated involving at least five representative high-power fields. The final positive cells were the mean of at least five different mice tumour tissues in each group. Data were presented as mean  $\pm$  SD. \*\*\* $p < 0.01$  compared to control group;  $\blacktriangle p < 0.05$  and  $\blacktriangle\blacktriangle\blacktriangle p < 0.001$  compared to gefitinib group. G: Gefitinib; Y: YYJDD.

nude mice. The results showed that the combination group exhibited a better inhibitory effect on tumour growth compared with the gefitinib group (Figure 5(A)). The tumour sizes in the combination group were much smaller ( $1630.66 \pm 208.30 \text{ mm}^3$  vs.  $1165.13 \pm 157.79 \text{ mm}^3$ ,  $p < 0.001$ ) and the weights were much lighter ( $0.56 \pm 0.09 \text{ g}$  vs.  $0.40 \pm 0.04 \text{ g}$ ,  $p < 0.05$ ) than those in gefitinib alone group (Figure 5(B,C)). Furthermore, there were no significant changes in the body weight of the mice in each group, suggesting that all the treatments were tolerable (Figure 5(D)). To further evaluate the apoptosis of tumour tissues in each group, TUNEL apoptosis detection was performed. As shown in Figure 5(E,F), the positive rate of TUNEL staining in tumour tissues was significantly increased by the combination treatment comparing with the control ( $1.65 \pm 0.29\%$  vs.  $22.33 \pm 2.75\%$ ,  $p < 0.001$ ) or gefitinib alone ( $7.37 \pm 0.87\%$  vs.  $22.33 \pm 2.75\%$ ,  $p < 0.001$ ). To determine whether the PI3K/Akt pathway was involved in the synergistic antitumor effect of YYJDD and gefitinib *in vivo*, we further applied immunohistochemistry analysis to detect the related protein expressions of Ki-67 and p-Akt. The

H-scores of Ki-67 and p-Akt were further reduced in presence of gefitinib plus YYJDD significantly (Figure 6(A-C)). Simultaneously, we extracted proteins from the tumour tissues. PI3K, p-PI3K, Akt and p-Akt were determined by western-blot assay. The significant decreased trend of p-PI3K/PI3K and p-Akt/Akt were found in combination treatment versus control or gefitinib group (Figure 6(D-F)), which was approximately consistent with the results *in vitro*. To sum up, these findings further emphasised YYJDD reduced gefitinib resistance in NSCLC via mediating the PI3K/Akt signalling pathway *in vivo*.

## Discussion

With the rapid development of precise targeted therapy, drug resistance to gefitinib is the main obstacle for the therapy of advanced NSCLC patients harbouring EGFR mutation. Its main mechanism can be described as two aspects: secondary mutation on EGFR and activation in the downstream pathways. Although

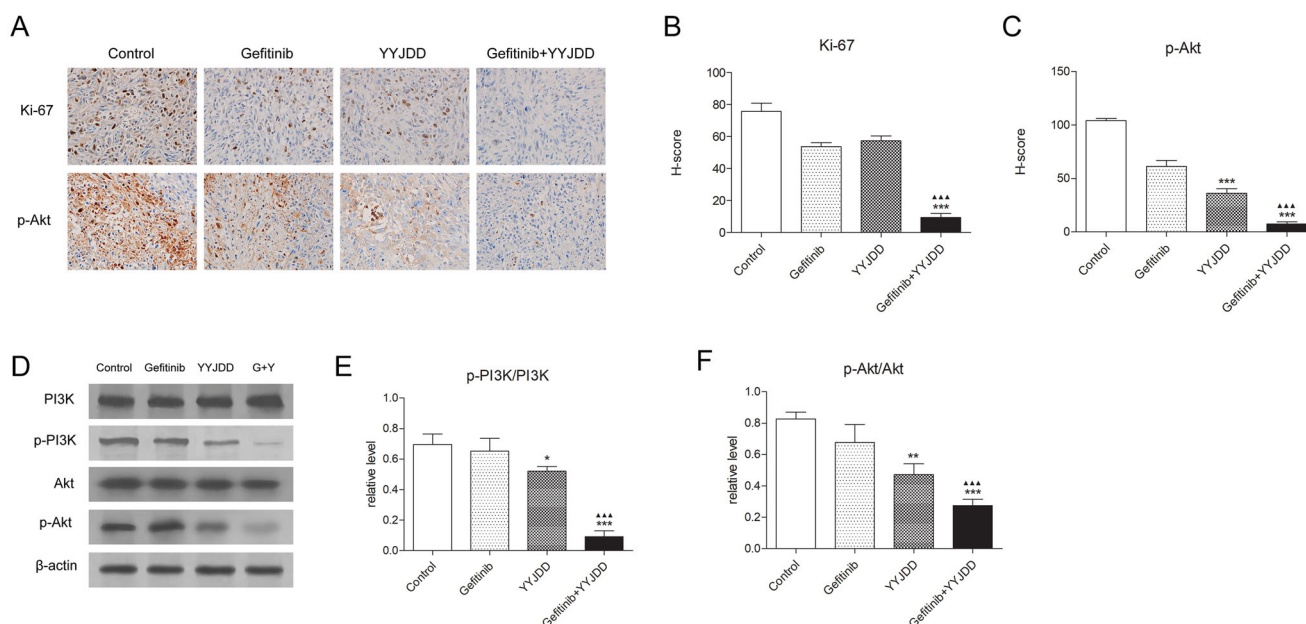


**Figure 6.** YYJDD overcame gefitinib resistance through the PI3K/Akt signalling pathway *in vivo*. (A) The expression of Ki-67 and p-Akt in tumour tissues of each group were detected by immunohistochemical staining. The level of protein expressions was estimated by counting at least 500 tumour cells in at least five representative high-power fields (original magnification,  $\times 400$ ). (B, C) The H-score of Ki-67 (B) and p-Akt (C) were calculated. (D) The protein expressions of PI3K, p-PI3K, Akt, and p-Akt in tumour tissues were determined by western-blot.  $\beta$ -actin was used as an internal control. (E, F) The relative level of p-PI3K/PI3K (E) and p-Akt/Akt (F) was calculated. Data were presented as mean  $\pm$  SD. The final statistical results were the mean of at least five different mice tumour tissues in each group. \* $p < 0.05$ , \*\* $p < 0.01$  and \*\*\* $p < 0.001$  versus control;  $\blacktriangle\blacktriangle\blacktriangle p < 0.001$  versus gefitinib. G: Gefitinib; Y: YYJDD.

strategies like the development of second or third generation of EGFR-TKIs have achieved certain curative effect, the problem of drug resistance still exists (Rotow and Bivona 2017). Therefore, gefitinib resistance has never been solved completely. Traditional Chinese medicine (TCM) has a long history and special characteristics of synergism and detoxification in overcoming drug resistance to targeted medicine. YYJDD has been widely used for treating NSCLC patients with oral EGFR-TKIs therapy in our daily medical activities. It consists of 8 Chinese medicines. Among them, *G. littoralis*, *O. japonicus*, *L. brownii* var. *viridulum*, and *D. nobile* can enhance immune response and strengthen lung (Meng et al. 2013; Zhu et al. 2015; Yang and Zhou 2019; Ge and Zhu 2020). *H. diffusa* is one of the most commonly-used Chinese herbs in anticancer prescriptions (Liu et al. 2013; Kuo et al. 2018). Some studies have confirmed that it could suppress tumour proliferation, migration and angiogenesis, etc. (Lin et al. 2013; Hu et al. 2015). *T. wallichiana* var. *mairei* has been reported to inhibit the proliferation and promote apoptosis of A549 cells, HeLa cells, etc. (Cui et al. 2015; Liu et al. 2016). *C. reticulata* has the effect of invigorating spleen and possesses wide pharmacological actions such as antioxidant, anti-inflammatory, and anticancer activities (Yu et al. 2018). *C. pilosula* is generally used to tonify spleen and lung. Its activities against gastric cancer, colon cancer, and hepatocellular carcinoma have been reported (Bailly 2021). In our clinical observation, we found that YYJDD could improve the ORR as well as reduce the side effects when combined with gefitinib. Based on the satisfactory curative effect, the underlying mechanism should be elucidated. Here in the present study, we firstly demonstrated that YYJDD markedly reduced gefitinib resistance via the PI3K/Akt signalling pathway *in vitro* and *in vivo*.

Based on the cell proliferation experimental data *in vitro*, treatment of H1975 cells with YYJDD or gefitinib alone resulted in only slight cell growth inhibition. While the combination treatment could significantly block the self-renewal of H1975

cells. *In vivo*, the tumour sizes of xenograft nude mice model in the combination group were much smaller than those in the control, YYJDD or gefitinib groups. Importantly, there was no significant difference in body weight among each group, indicating that this strategy had no significant systemic toxicity. Hence, YYJDD might become an ideal candidate against gefitinib resistance due to its efficacy and safety. It was essential to understand its mechanism.

Due to the significant cell inhibition enhanced by YYJDD combined with gefitinib, we wondered whether apoptosis was involved in this process. Apoptosis, also known as programmed cell death, refers to the spontaneous and orderly death of cells controlled by genes to maintain homeostasis (Wong 2011). Inhibition of apoptosis is considered to be a vital step in the development of EGFR-TKI resistance. Modern research indicated that the apoptotic response of resistant NSCLC cells to EGFR-TKIs was weakened (Hata et al. 2016). Thus, apoptosis induction plays an important role in modern cancer therapy (Carneiro and El-Deiry 2020). In this study, the apoptosis was detected by flow cytometry detection *in vitro* and by TUNEL assay *in vivo*. The *in vitro* results revealed that YYJDD enhanced the efficacy of gefitinib to induce apoptosis with the increased protein expression level of cleaved caspase-3 and cleaved PARP in H1975 cells. Meanwhile, our *in vivo* results indicated the positive rate of TUNEL staining in tumour tissues induced by gefitinib was further increased in the presence of YYJDD. Caspase-3, which can specifically catalyse the cleavage of many important cellular proteins, is a critical regulator of apoptosis. It is mainly responsible for cleaving PARP at a highly evolutionarily conserved cleavage site. PARP is related to DNA repair and gene integrity. Caspase-3 can recognise the Asp-Glu-Val-Asp (DVCD) sequence in PARP and cut it. The cleavage of PARP results in the loss of normal function and activation of the endonuclease. Then the degradation of DNA among nucleosomes will occur, leading to apoptosis (Virág and Szabó 2002). As the present study

demonstrated, apoptosis might be mainly responsible for YYJDD resensitizing H1975 cells to gefitinib.

The PI3K/Akt signalling pathway is involved in tumorigenesis, cancer progression, drug resistance, etc. (Yip 2015; Liu et al. 2020; Tan 2020; Cao et al. 2020). The reactivation of the PI3K/Akt pathway was discovered in patients with drug resistance to EGFR-TKIs (Liu et al. 2018). Other literature also pointed out that even under the pressure of gefitinib, the PI3K/Akt pathway was reactivated in H1975 cells, indicating that the reactivation of the PI3K/Akt pathway might lead to gefitinib resistance (Chen et al. 2018). Activated PI3K initiates the activation and phosphorylation of a key downstream kinase-Akt. Phosphorylated Akt can inhibit a series of apoptosis-related proteins by regulating the downstream signalling molecules so as to protect the caspase cascade and suppress apoptosis activity (Iida et al. 2020). Due to its relationship with drug resistance, the PI3K/Akt signalling pathway has attracted extensive attention as a potential target for antitumor therapeutic strategy (Tan 2020). Down-regulation of this signalling pathway might lead to cellular apoptosis and sensitisation to anticancer therapy (Yip 2015; Tan 2020). Hence, we detected the effect of YYJDD combined with gefitinib on the PI3K/Akt pathway by western-blot analysis. We found that gefitinib had no effect on the expression of p-PI3K and p-Akt in H1975 cells, which was consistent with the literature (Chen et al. 2018). Meanwhile, the expressions of p-PI3K and p-Akt were reduced under the pressure of YYJDD or combination treatment. The results were highly in accordance with the present study *in vivo* which were revealed by immunohistochemistry analysis and western-blot assay, suggesting that YYJDD and combination treatment could inhibit the PI3K/Akt pathway.

Evidence indicated that relieving the regulation of the PI3K/Akt pathway could promote drug resistance in NSCLC. The application of PI3K inhibitors, such as LY294002, could induce the apoptosis of the gefitinib-resistance cell line and increase the sensitivity of EGFR-TKI therapy (Li et al. 2011). As we know, LY294002 could block PI3K and inactivate Akt phosphorylation, leading to cell growth inhibition and apoptosis. To further uncover the role of the PI3K/Akt pathway on apoptosis induced by YYJDD combined with gefitinib, we added LY294002 to YYJDD or combination treatment. The data showed that LY294002 could inhibit the proliferation, promote apoptosis and suppress the ratio of p-Akt/Akt. Further, co-treatment of LY294002 with YYJDD or combination therapy had superior effects than treatments with either one alone. Hence, the positive activity of YYJDD on gefitinib-resistance was dependent on the PI3K/Akt pathway. By analysing the regulatory relationship between apoptotic proteins and the PI3K/Akt pathway, we found that the increased level of cleaved caspase-3 and cleaved PARP induced by combination treatment was accompanied by the inhibition of the PI3K/Akt. Blocking the PI3K/Akt pathway with LY294002 could further increase YYJDD or combination-induced cell apoptosis. That is to say, the increase of apoptotic proteins was induced by the suppression of the PI3K/Akt. Therefore, we concluded that YYJDD enhanced the sensitivity of gefitinib to H1975 by inducing apoptosis through the PI3K/Akt pathway.

After reviewing the results of this study, it is necessary for us to focus on the active ingredients in YYJDD again. In this study, some chemical compounds of YYJDD were identified by HPLC analysis. Based on the previous evidence, hesperidin could induce apoptosis through the PI3K/Akt pathway to prevent colon carcinogenesis (Saiprasad et al. 2014). It could also act the protective effect against a chemically induced liver cancer through the PI3K/Akt pathway (Mo'men et al. 2019). Dioscin could suppress

the viability of various cancer cells (ovarian cancer, lung cancer, gallbladder, etc.) by regulating the PI3K/Akt pathway (Song et al. 2017; Guo and Ding 2018; Mao et al. 2020). Lobetyolin was proven that its inhibitory effect on breast cancer cells was related to Akt (Chen et al. 2021). The efficacy of YYJDD overcoming gefitinib resistance via the PI3K/Akt pathway might be attributed to these active ingredients to a certain extent. Nevertheless, more precise research needs to be done in the future.

However, in the present study, there still exists some limitations. Firstly, we roughly speculated that YYJDD could enhance the sensitivity of gefitinib to resistant cell lines via apoptosis, while lacking of the specific apoptotic pathway (the extrinsic or intrinsic pathway). Secondly, we only focussed on the role of the PI3K/Akt pathway in YYJDD resensitizing H1975 to gefitinib, the specific target, and the role of some other important pathways (such as MAPK or STAT signalling pathway) still remain unclear. Thirdly, we should further explore the definite mechanism of the main active compounds in YYJDD. Therefore, the above limitations need to be explored in our future investigations.

## Conclusion

Our investigation demonstrated that YYJDD enhanced the effect of gefitinib in H1975 cells. The mechanism of YYJDD reducing gefitinib resistance was achieved by inducing apoptosis via down-regulation of the PI3K/Akt signalling pathway. Therefore, YYJDD combined with gefitinib might be an alternative therapeutic strategy for the treatment of drug resistance induced by the first generation of EGFR-TKIs in NSCLC.

## Disclosure statement

No potential conflict of interest was reported by the author(s).

## Funding

This work was supported by the National Natural Science Foundation of China under Grant [number: 81704013]; Clinical (gastric cancer) Cooperation Pilot Project of Chinese and Western Medicine for Major and Difficult Diseases; The Key Research and Development Projects of Science and Technology Department of Zhejiang Province under Grant [number: 2015C03G2120026]; and Zhejiang Traditional Chinese Medicine of Science and Technology Program under Grant [number: 2020ZA053].

## Data availability statement

The data that support the findings of this study are available on reasonable request from the corresponding author.

## References

- Bailey C. 2021. Anticancer properties of lobetyolin, an essential component of *Radix Codonopsis* (Dangshen). *Nat Prod Bioprospect*. 11(2):143–153.
- Bray F, Ferlay J, Soerjomataram I, Siegel RL, Torre LA, Jemal A. 2018. Global cancer statistics 2018: GLOBOCAN estimates of incidence and mortality worldwide for 36 cancers in 185 countries. *CA Cancer J Clin*. 68(6):394–424.
- Cao S, Li L, Li J, Zhao H. 2020. MiR-1299 impedes the progression of non-small-cell lung cancer through EGFR/PI3K/Akt signaling pathway. *Oncotargets Ther*. 13:7493–7502.

- Carneiro BA, El-Deiry WS. 2020. Targeting apoptosis in cancer therapy. *Nat Rev Clin Oncol.* 17(7):395–417.
- Chen Q, Pan Z, Zhao M, Wang Q, Qiao C, Miao L, Ding X. 2018. High cholesterol in lipid rafts reduces the sensitivity to EGFR-TKI therapy in non-small cell lung cancer. *J Cell Physiol.* 233(9):6722–6732.
- Chen Y, Tian Y, Jin G, Cui Z, Guo W, Zhang X, Liu X. 2021. Lobetyolin inhibits the proliferation of breast cancer cells via ASCT2 down-regulation-induced apoptosis. *Hum Exp Toxicol.* <https://doi.org/10.1177/09603271211021476>.
- Chou TC. 2006. Theoretical basis, experimental design, and computerized simulation of synergism and antagonism in drug combination studies. *Pharmacol Rev.* 58(3):621–681.
- Chou TC. 2010. Drug combination studies and their synergy quantification using the Chou-Talalay method. *Cancer Res.* 70(2):440–446.
- Cui QL, Ye P, Shu QJ, Shao M. 2015. Study on inhibitory effect of aqueous extract of *Taxus Chinensis* var. *mairei* combined erlotinib on A549 xenograft in nude mice and its mechanism. *Zhongguo Zhong Xi Yi Jie He Za Zhi.* 35:572–577.
- Ge HB, Zhu J. 2020. Clinical efficacy of Baihe Gujin decoction combined with anti-tuberculosis therapy for pulmonary tuberculosis with yin-deficiency and fire-hyperactivity syndrome. *J Int Med Res.* 48(5):300060519875535.
- Gendreau SB, Ventura R, Keast P, Laird AD, Yakes FM, Zhang W, Bentzien F, Cancilla B, Lutman J, Chu F, et al. 2007. Inhibition of the T790M gatekeeper mutant of the epidermal growth factor receptor by EXEL-7647. *Clin Cancer Res.* 13(12):3713–3723.
- Guo X, Ding X. 2018. Dioscin suppresses the viability of ovarian cancer cells by regulating the VEGFR2 and PI3K/Akt/MAPK signaling pathways. *Oncol Lett.* 15(6):9537–9542.
- Hata AN, Niederst MJ, Archibald HL, Gomez-Caraballo M, Siddiqui FM, Mulvey HE, Maruvka YE, Ji F, Bhang HE, Krishnamurthy Radhakrishna V, et al. 2016. Tumor cells can follow distinct evolutionary paths to become resistant to epidermal growth factor receptor inhibition. *Nat Med.* 22(3):262–269.
- Heigener DF, Reck M. 2018. Lung cancer in 2017: giant steps and stumbling blocks. *Nat Rev Clin Oncol.* 15(2):71–72.
- Hu E, Wang D, Chen J, Tao X. 2015. Novel cyclotides from *Hedyotis diffusa* induce apoptosis and inhibit proliferation and migration of prostate cancer cells. *Int J Clin Exp Med.* 8(3):4059–4065.
- Iida M, Harari PM, Wheeler DL, Toulany M. 2020. Targeting AKT/PKB to improve treatment outcomes for solid tumors. *Mutat Res.* 819–820:111690.
- Jiao L, Xu J, Sun J, Chen Z, Gong Y, Bi L, Lu Y, Yao J, Zhu W, Hou A, et al. 2019. Chinese herbal medicine combined with EGFR-TKI in EGFR mutation-positive advanced pulmonary adenocarcinoma (CATLA): a multicenter, randomized, double-blind, placebo-controlled trial. *Front Pharmacol.* 10:732.
- Kuo YT, Liao HH, Chiang JH, Wu MY, Chen BC, Chang CM, Yeh MH, Chang TT, Sun MF, Yeh CC, et al. 2018. Complementary Chinese herbal medicine therapy improves survival of patients with pancreatic cancer in Taiwan: a nationwide population-based cohort study. *Integr Cancer Ther.* 17(2):411–422.
- Larsen AK, Ouaret D, El Ouardani K, Petitprez A. 2011. Targeting EGFR and VEGF(R) pathway cross-talk in tumor survival and angiogenesis. *Pharmacol Ther.* 131(1):80–90.
- Li GY. 2017. Clinical observation on the treatment of lung adenocarcinoma of Ying-xu-du-yun type IIIb-IV EGFR mutant with nourishing yin and detoxifying prescription decoction combined with icotinib [master's thesis]. Hangzhou (ZJ): Zhejiang Chinese Medical University.
- Li H, Schmid-Bindert G, Wang D, Zhao Y, Yang X, Su B, Zhou C. 2011. Blocking the PI3K/AKT and MEK/ERK signaling pathways can overcome gefitinib-resistance in non-small cell lung cancer cell lines. *Adv Med Sci.* 56(2):275–284.
- Li L, Wang S, Zheng F, Wu W, Hann SS. 2016. Chinese herbal medicine Fuzheng Kang-Ai decoction sensitized the effect of gefitinib on inhibition of human lung cancer cells through inactivating PI3-K/Akt-mediated suppressing MUC1 expression. *J Ethnopharmacol.* 194:918–929.
- Lin J, Wei L, Shen A, Cai Q, Xu W, Li H, Zhan Y, Hong Z, Peng J. 2013. *Hedyotis diffusa* Willd extract suppresses Sonic hedgehog signaling leading to the inhibition of colorectal cancer ctal cancer angiogenesis. *Int J Oncol.* 42(2):651–666.
- Liu HS, Gao YH, Liu LH, Liu W, Shi QW, Dong M, Suzuki T, Kiyota H. 2016. Inhibitory effect of 13 taxane diterpenoids from Chinese yew (*Taxus chinensis* var. *mairei*) on the proliferation of HeLa cervical cancer cells. *Biosci Biotechnol Biochem.* 80(10):1883–1886.
- Liu Q, Yu S, Zhao W, Qin S, Chu Q, Wu K. 2018. EGFR-TKIs resistance via EGFR-independent signaling pathways. *Mol Cancer.* 17(1):53.
- Liu X, Jiang T, Li X, Zhao C, Li J, Zhou F, Zhang L, Zhao S, Jia Y, Shi J, et al. 2020. Exosomes transmit T790M mutation-induced resistance in EGFR-mutant NSCLC by activating the PI3K/AKT signalling pathway. *J Cell Mol Med.* 24(2):1529–1540.
- Liu Z, Chen S, Cai J, Zhang E, Lan L, Zheng J, Liao L, Yang X, Zhou C, Du J. 2013. Traditional Chinese medicine syndrome-related herbal prescriptions in treatment of malignant tumors. *J Tradit Chin Med.* 33(1):19–26.
- Liu Z, Sun X, Liu H, Ma T, Shi J, Jia B, Zhao H, Wang F. 2014. Early assessment of tumor response to gefitinib treatment by noninvasive optical imaging of tumor vascular endothelial growth factor expression in animal models. *J Nucl Med.* 55(5):818–823.
- Ludovini V, Bianconi F, Pistola L, Chiari R, Minotti V, Colella R, Giuffrida D, Tofanetti FR, Siggillino A, Flacco A, et al. 2011. Phosphoinositide-3-kinase catalytic alpha and KRAS mutations are important predictors of resistance to therapy with epidermal growth factor receptor tyrosine kinase inhibitors in patients with advanced non-small cell lung cancer. *J Thorac Oncol.* 6(4):707–715.
- Mao W, Yin H, Chen W, Zhao T, Wu S, Jin H, Du B, Tan Y, Zhang R, He Y. 2020. Network pharmacology and experimental evidence reveal dioscin suppresses proliferation, invasion, and EMT via Akt/GSK3b/mTOR signaling in lung adenocarcinoma. *Drug Des Devel Ther.* 14:2135–2147.
- Maređziak M, Tomaszewski K, Polinceusz P, Lewandowski D, Marycz K. 2017. Static magnetic field enhances the viability and proliferation rate of adipose tissue-derived mesenchymal stem cells potentially through activation of the phosphoinositide 3-kinase/Akt (the PI3K/Akt) pathway. *Electromagn Biol Med.* 36(1):45–54.
- Meng LZ, Lv GP, Hu DJ, Cheong KL, Xie J, Zhao J, Li SP. 2013. Effects of polysaccharides from different species of *Dendrobium* (Shihu) on macrophage function. *Molecules.* 18(5):5779–5791.
- Mitsudomi T, Morita S, Yatabe Y, Negoro S, Okamoto I, Tsurutani J, Seto T, Satouchi M, Tada H, Hirashima T, et al. 2010. Gefitinib versus cisplatin plus docetaxel in patients with non-small-cell lung cancer harbouring mutations of the epidermal growth factor receptor (WJTOG3405): an open label, randomised phase 3 trial. *Lancet Oncol.* 11(2):121–128.
- Mok TS, Wu YL, Thongprasert S, Yang CH, Chu DT, Saijo N, Sunpaweravong P, Han B, Margono B, Ichinose Y, et al. 2009. Gefitinib or carboplatin-paclitaxel in pulmonary adenocarcinoma. *N Engl J Med.* 361(10):947–957.
- Mo'men YS, Hussein RM, Kandeil MA. 2019. Involvement of the PI3K/Akt pathway in the protective effect of hesperidin against a chemically induced liver cancer in rats. *J Biochem Mol Toxicol.* 33(6):e22305.
- Normanno N, Maiello MR, Chicchinelli N, Iannaccone A, Esposito C, De Cecio R, D'alessio A, De Luca A. 2017. Targeting the EGFR T790M mutation in non-small-cell lung cancer. *Expert Opin Ther Targets.* 21(2):159–165.
- Patil VM, Noronha V, Joshi A, Choughule AB, Bhattacharjee A, Kumar R, Goud S, More S, Ramaswamy A, Karpe A, et al. 2017. Phase III study of gefitinib or pemetrexed with carboplatin in EGFR-mutated advanced lung adenocarcinoma. *ESMO Open.* 2(1):e000168.
- Rotow J, Bivona TG. 2017. Understanding and targeting resistance mechanisms in NSCLC. *Nat Rev Cancer.* 17(11):637–658.
- Saiprasad G, Chitra P, Manikandan R, Sudhandiran G. 2014. Hesperidin induces apoptosis and triggers autophagic markers through inhibition of Aurora-A mediated phosphoinositide-3-kinase/Akt/mammalian target of rapamycin and glycogen synthase kinase-3 beta signalling cascades in experimental colon carcinogenesis. *Eur J Cancer.* 50(14):2489–2507.
- Sato H, Yamamoto H, Sakaguchi M, Shien K, Tomida S, Shien T, Ikeda H, Hatono M, Torigoe H, Namba K, et al. 2018. Combined inhibition of MEK and PI3K pathways overcomes acquired resistance to EGFR-TKIs in non-small cell lung cancer. *Cancer Sci.* 109(10):3183–3196.
- Song X, Wang Z, Liang H, Zhang W, Ye Y, Li H, Hu Y, Zhang Y, Weng H, Lu J, et al. 2017. Dioscin induces gallbladder cancer apoptosis by inhibiting ROS-mediated PI3K/Akt signalling. *Int J Biol Sci.* 13(6):782–793.
- Tan AC. 2020. Targeting the PI3K/Akt/mTOR pathway in non-small cell lung cancer (NSCLC). *Thorac Cancer.* 11(3):511–518.
- Turke AB, Zejnullahu K, Wu YL, Song Y, Dias-Santagata D, Lifshits E, Toschi L, Rogers A, Mok T, Sequist L, et al. 2010. Preexistence and clonal selection of MET amplification in EGFR mutant NSCLC. *Cancer Cell.* 17(1):77–88.

- Virág L, Szabó C. 2002. The therapeutic potential of poly(ADP-ribose) polymerase inhibitors. *Pharmacol Rev.* 54(3):375–429.
- Wei W, Wu XM, Li YJ. 2010. *Yao Li Shi Yan Fang Fa Xue* [Methodology of Pharmacological Experiment]. 4th ed. Beijing: People's Medical Publishing House.
- Wong RS. 2011. Apoptosis in cancer: from pathogenesis to treatment. *J Exp Clin Cancer Res.* 30:87.
- Wu H, Fan F, Liu Z, Shen C, Wang A, Lu Y. 2015. Norcantharidin combined with EGFR-TKIs overcomes HGF-induced resistance to EGFR-TKIs in EGFR mutant lung cancer cells via inhibition of Met/PI3k/Akt pathway. *Cancer Chemother Pharmacol.* 76(2):307–315.
- Yang Y, Zhou Y. 2019. Shashen-Maidong decoction-mediated IFN- $\gamma$  and IL-4 on the regulation of Th1/Th2 imbalance in RP rats. *Biomed Res Int.* 2019:1–7.
- Yip PY. 2015. Phosphatidylinositol 3-kinase-AKT-mammalian target of rapamycin (PI3K-Akt-mTOR) signaling pathway in non-small cell lung cancer. *Transl Lung Cancer Res.* 4(2):165–176.
- Yu X, Sun S, Guo Y, Liu Y, Yang D, Li G, Lü S. 2018. *Citri Reticulatae* Pericarpium (Chenpi): Botany, ethnopharmacology, phytochemistry, and pharmacology of a frequently used traditional Chinese medicine. *J Ethnopharmacol.* 220:265–282.
- Zhu X, Zhang Y, Liu X, Hou D, Gao T. 2015. Authentication of commercial processed *Glehniae Radix* (Beishashen) by DNA barcodes. *Chin Med.* 10:35.